

A Vehicle Position Estimation Method Combining Roadside Vehicle Detector and In-Vehicle Sensors

Shunya Yamada

Yousuke Watanabe

Hiroaki Takada

Graduate School of Informatics
Nagoya University
Nagoya, Japan 464-8601
Email: s_yamada@ertl.jp

Institutes of Innovation for Future Society
Nagoya University
Nagoya, Japan 464-8601
Email: watanabe@coi.nagoya-u.ac.jp

Institutes of Innovation for Future Society
and graduate School of Informatics
Nagoya University
Nagoya, Japan 464-8601
Email: hiro@ertl.jp

Abstract—To improve highway traffic safety and traffic flow, it is important to properly manage merging at junctions. Accurate vehicle positions and velocities are necessary to achieve this, but existing sensors have both advantages and disadvantages. Roadside vehicle detectors are very accurate, but only available at fixed points. By contrast, in-vehicle Global Navigation Satellite System (GNSS) sensors can be used anywhere except in tunnels, but are less accurate. However these sensors can compensate for each other's weak points. In this paper, we proposed a vehicle position estimation method that combines roadside vehicle detector and in-vehicle sensors. This gathers data from roadside vehicle detector and in-vehicle sensors via different wireless networks, applies Kalman filters to calculate accurate position and velocity. When exchanging information over wireless networks, communication delays occur and data arrival sequence is not guaranteed. Our method can retroactively calculate vehicle position in the presence of delays below a maximum acceptable threshold. The results of simulation experiments show that our method can estimate vehicle positions more accurately than using data from either sensor alone.

Keywords—Sensor fusion, Position estimation, Communication delays, DSRC, Intelligent transportation system.

I. INTRODUCTION

At highway junctions, vehicles merging into the main lane are increasingly causing the traffic congestion in that lane [1], and the 20-30% of highway truck accidents occur at or near junctions [2]. Thus, appropriately managing traffic and controlling merging at junctions is important for improving both highway safety and traffic flow.

Several previous studies have investigated proper traffic management and merging control at junctions. Cui et al. [3] proposed a system for detecting collisions by estimating the vehicle arrival time at junctions. Their system obtain the vehicle positions and velocities from a monocular camera installed at the junction and uses these to estimate the arrival times. Milanés et al. [4], local control system installed near the junction receives position and velocity information from approaching vehicles and send them a low-risk merging strategies. Chou et al. [5] proposed a merging method based on Vehicle-to-Vehicle (V2V) communication. Vehicles approaching the junction use this to exchange their positions and velocities, then the vehicles in the main lane create gaps for entering vehicles before they have even reached the merging point. Hirai et al. [6] proposed such a system that used roadside vehicle detection sensors, installed before merging points. Roadside vehicle detection sensors are often used to get presence of vehicles and vehicles'

velocities on the lane in order to estimate traffic flows (see Figure 1). In Hirai's approach, these are used to acquire vehicles' velocities and estimate their arrival times at the merging points. When a vehicle on the on-ramp will arrive at almost the same time as a vehicle in the main lane, the system alerts the vehicle in main lane, enabling to prepare for merging even if its driver has not seen the vehicle on the on-ramp. Giving drivers longer to prepare makes the process safe. Japan's government started the field tests of autonomous driving in Tokyo waterfront area [7] and roadside vehicle detection sensors' information can be available in the filed tests. Proper traffic management and merging control at junctions are considered by participating companies in the filed tests.

All of these merging methods depend on vehicle position and velocity information to properly manage traffic and control



Figure 1. Roadside vehicle detection sensor.

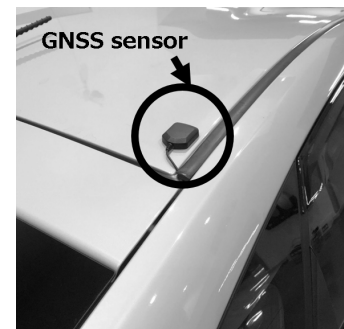


Figure 2. General-purpose GNSS sensor.

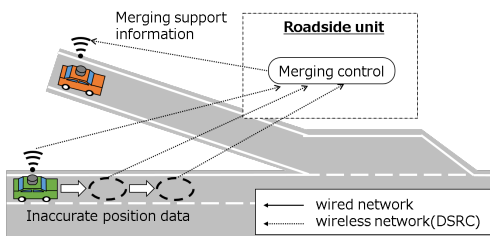


Figure 3. Existing approach1: Using GNSS sensors.

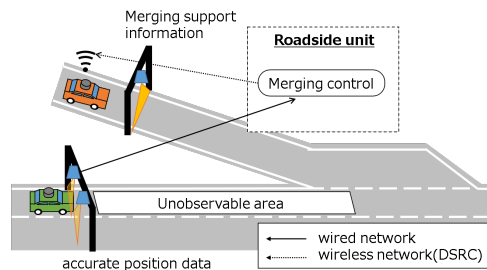


Figure 4. Existing approach2: Using roadside vehicle detection sensors.

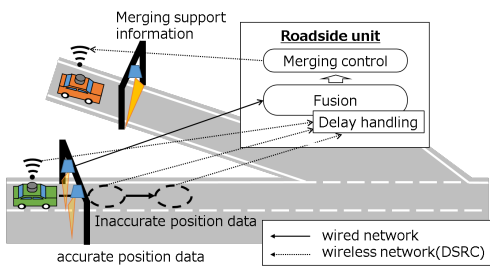


Figure 5. Proposed approach: Combining both sensors.

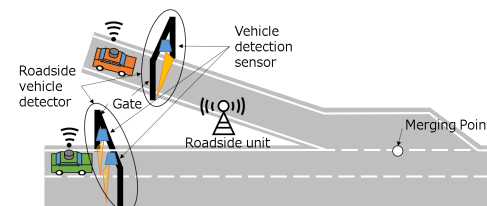


Figure 6. Merging support system overview.

merging at junctions. The location estimation method using a camera needs to be installed so that occlusion does not occur, so the place where it can be used is limited. Although accurate vehicle velocities can be obtained from speed sensors, vehicle positions can be incorrect. These are often acquired from position estimation methods using a Light Detection and Ranging (LiDAR) or in-vehicle Global Navigation Satellite System (GNSS) sensors. Since the position estimation method using a LiDAR can estimate the position more accurately than GNSS sensors, autonomous vehicles often use it for position estimation. However, a cost of LiDAR is much higher than general-purpose GNSS sensors and a LiDAR will not be installed immediately in conventional vehicles. GNSS sensors are often used to get position and accurate time by receiving signals emitted from satellites. These can function anywhere except in tunnels. Signals received from satellites contain noise. Since high-precision GNSS sensors can correct noise [8], they can obtain accurate positions but they are very expensive. GNSS sensors mounted on vehicles are almost general-purpose products (see Figure 2). They are cheap but positions measured via them can, depending on the location, differ from the true position by more than 10 meters. It has been confirmed that properly manage traffic and control merging control at junctions cannot be performed when vehicles' position errors are large [5]. The system using roadside vehicle detection sensors' estimates the vehicle arrival times accurately when the sensor is close to the merging point. However, the error increases with the distance between the sensor and the merging point. Moreover, establishment cost is high and multiple installations are not reasonable because roadside vehicle detection sensors are usually attached to poles installed at roadsides and gates across the road (see Figure 1).

The errors in GNSS-based vehicle positions are almost constant, except in areas where the environment is changing rapidly. On the other hand, the errors in the positions estimated by roadside vehicle detection sensors are small, as long as the sensor is close to the merging point, but they increase

with the sensor's distance from the merging point, leading to large errors in the estimated vehicle arrival times. Thus, we consider an approach that combines the positions obtained from GNSS and roadside vehicle detection sensors. In this way, we obtain accurate positions near the roadside vehicle detection sensors but the error does not increase too much when the roadside vehicle detection sensor is further from the merging points. Position estimation method using both GNSS and roadside vehicle detection sensors has not been considered because roadside vehicle detection sensors are infrastructure sensors and cannot be easily used unlike GNSS sensors. For example, these have been managed by National Police Agency in Japan and data from these can only be acquired at specific authorized locations.

In addition, Dedicated Short-Range Communications (DSRC) or Long Term Evolution (LTE) are used for V2V and Vehicle-to-Infrastructure (V2I) communications. However, exchanging information via such wireless networks leads to communication delays. According to Dey et al. [9], these are approximately 1.5[s] for LTE and 100[ms] for DSRC (for communication between a vehicle traveling at 80[km/s] and a roadside unit). These delays also mean the data arrival times are not guaranteed. Thus, we believe that we obtain more accurate vehicle positions by combining data from GNSS and roadside vehicle detection sensors and compensating for communication delays.

In this paper, we propose a vehicle position estimation method that combines data from roadside vehicle detector and in-vehicle sensors. This can retroactively calculate prior vehicle positions in the presence of delays below the maximum acceptable threshold. This paper makes the following two main contributions.

- 1) A vehicle position estimation method that combines data from roadside vehicle detector and in-vehicle sensors.
- 2) A communication delays compensation method.

1) In our system, a vehicle detection sensor is installed before the merging point and a roadside unit is installed near the junction. In-vehicle sensor information is used to estimate its position and velocity. In addition, a roadside vehicle detection sensor is also used to estimate the vehicle position based on the sensor position and vehicle velocity. The two estimates are combined using a statistical approach proposed by Duffin [10]. Previous studies used only one of position information obtained from GNSS and roadside vehicle detection sensors (see Figures 3 and 4). However, our method estimates positions using both position information (see Figure 5).

2) Vehicle positions at earlier times are retroactively calculated when older data arrives, up to the predetermined maximum communication delay. When the roadside unit does not receive information from a vehicle, it estimates the vehicle's position based on the most recent information received from it. Modified Kalman filters that take communication delays into accounts has been proposed [11]. The second contribution of this paper is applying the modified Kalman filter to the scene of merging support.

This paper is organized as follows. Section II describes the assumptions made in this study. Section III introduces the proposed method. Section IV evaluates the method using simulations, and then Section V presents results. Section VI concludes the paper.

II. ASSUMPTIONS

In this study, vehicle detection sensors (mounted in gates) are installed before the merging point and a roadside unit is located near the junction (see Figure 6). All vehicles have GNSS devices, speed sensors, and DSRC communication devices. The communication range of DSRC is fixed. Its communication area is limited in a hot spot. On the other hand, DSRC has the advantage that the number of vehicles simultaneously communicated with a roadside unit does not become overcapacity because of the limited communication area. Vehicles approaching the junction send their current position and velocity, as well as the time the data was acquired, to the roadside unit via DSRC. This information is repeatedly sent at regular intervals within DSRC range and started to send before the vehicle passes through the gate.

The vehicle positions and velocities are given in terms of the average value and standard deviation. The vehicle detection sensors are assumed to obtain the positions of the vehicle's center. The system clocks in the vehicles, roadside vehicle detector, and roadside units are assumed to be synchronized. There is some delay in the communications between vehicles and roadside units. On the other hand, the communication delays between the roadside vehicle detector and roadside unit are assumed to be negligible because the communication between them is via wire and dedicated connection. Finally, we consider lateral movement but not vertical movement.

Figure 7 shows the environmental model used in this study. Here, the vehicle drives from the start point toward the merging point. A roadside vehicle detector is installed at $x = x_0^{rzd}$ [m]. The vehicle sends information about its position (namely the average x_t^{gps} [m] and standard deviation σ_t^{gps} [m]) and velocity (average v_t [km/s] and standard deviation σ_{v_t} [km/s]) to the roadside unit. Meanwhile, the roadside vehicle detector sends the position of the vehicle's center (average x_0^{rzd} [m] and standard deviation σ_0^{rzd} [m]) and the detection time t_0 [s] to the roadside unit when the vehicle passes through the gate.

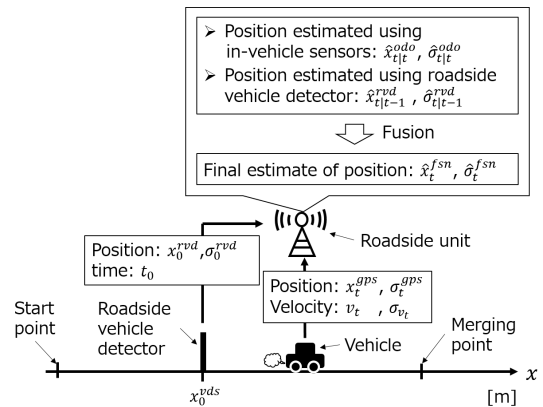


Figure 7. Illustration of the position estimation model and variable definitions.

The roadside unit estimates the vehicle's position, both using the information received from the vehicle (average $\hat{x}_{t|t}^{odo}$ [m] and standard deviation $\hat{\sigma}_{t|t}^{odo}$ [m]) and using that from the roadside vehicular detector (average $\hat{x}_{t|t-1}^{rzd}$ [m] and standard deviation $\hat{\sigma}_{t|t-1}^{rzd}$ [m]). Then, it combines these two estimates to obtain the final vehicle position (average \hat{x}_t^{fsn} [m] and standard deviation $\hat{\sigma}_t^{fsn}$ [m]).

The assumptions in this study came from actual field test of Japan [7]. Support for autonomous driving by providing information for automatically adjusting the speed and timing of entering the main line at highway junctions has been considered in the field tests [12]. These information is provided from roadside units installed near the vehicle detection sensors via DSRC. Roadside units estimate the speed and timing to safely join the main lane from the vehicle velocity obtained from the vehicle detection sensors. Furthermore, there are already previous studies on time synchronization [13]. Therefore, these assumptions are realistic.

III. PROPOSED METHOD

In this section, we described our proposed position estimation approach, followed by our method of compensating for communication delays.

A. Position Estimation

Vehicle approaching the merging point send their position and velocity information to the roadside unit via DSRC. This applies Kalman filters to the data to estimate each vehicle's position before it passes through the gate. When the vehicle passes through the gate, the roadside unit also receives the estimated position of vehicle's center from roadside vehicle detector. The roadside unit produces a final estimate of vehicle's position by combining its estimated center and velocity with the Kalman filters' prediction using a statistical approach proposed by Duffin [10].

Figure 8 presents a flow diagram showing the steps performed to estimate the vehicle's position when it passes through the gate at time t_0 [s]. Here, the vehicle's position is estimated by applying Kalman filters to the position and velocity information received from it until passes through the gate. Kalman filters are often used to estimates the exact state based on inaccurate, noisy information, hence, we use it here to estimate the vehicle position from noisy position and velocity

information.

Kalman filters are divided into prediction and correction steps. During the prediction step, the vehicle's position is estimated based on the estimate from the previous time step and the current vehicle velocity information. The correction step adjusts this estimated position using the current vehicle position information. The specific equations are as follows.

Prediction step:

$$\hat{x}_{t|t-1}^{odo} = \hat{x}_{t-1|t-1}^{odo} + \frac{5}{18}v_t dt, \quad (1)$$

$$\left(\hat{\sigma}_{t|t-1}^{odo}\right)^2 = \left(\hat{\sigma}_{t-1|t-1}^{odo}\right)^2 + \left(\frac{5}{18}\sigma_{v_t} dt\right)^2. \quad (2)$$

Correction step:

$$\hat{x}_{t|t}^{odo} = \hat{x}_{t|t-1}^{odo} + k_t \left(x_t^{gps} - \hat{x}_{t|t-1}^{odo}\right), \quad (3)$$

$$\left(\hat{\sigma}_{t|t}^{odo}\right)^2 = (1 - k_t) \left(\hat{\sigma}_{t|t-1}^{odo}\right)^2, \quad (4)$$

$$k_t = \frac{\left(\hat{\sigma}_{t|t-1}^{odo}\right)^2}{\left\{\left(\hat{\sigma}_{t|t-1}^{odo}\right)^2 + \left(\sigma_t^{gps}\right)^2\right\}}. \quad (5)$$

where $\hat{x}_{t|t-1}^{odo}$ [m] and $\hat{\sigma}_{t|t-1}^{odo}$ [m] are the average and standard deviation of the vehicle position predicted by the Kalman filters at timestep t [s], and $\hat{x}_{t|t}^{odo}$ [m] and $\hat{\sigma}_{t|t}^{odo}$ [m] are the average and standard deviation of the vehicle position, respectively, generated by the correction step for timestep t [s], v_t [km/s] and σ_{v_t} [km/s] are the average and standard deviation of the vehicle velocity, respectively, generated by the correction step for timestep t [s], k_t is the Kalman gain at timestep t [s], and $\frac{5}{18}$ is a term to convert the vehicle velocity from [km/h] to [m/s].

The roadside unit receives the position of the vehicle's center from the roadside vehicle detector at time t_0 [s], then combines this with the velocity information received from the vehicle, and the Kalman filters' prediction step in order to estimate the vehicle's position. The specific equations are as follows.

Position estimation:

$$\hat{x}_t^{rvd} = \hat{x}_{t-1}^{rvd} + \frac{5}{18}v_t dt, \quad (6)$$

$$\left(\hat{\sigma}_t^{rvd}\right)^2 = \left(\hat{\sigma}_{t-1}^{rvd}\right)^2 + \left(\frac{5}{18}\sigma_{v_t} dt\right)^2. \quad (7)$$

where $\hat{x}_{t|t-1}^{rvd}$ [m] and $\hat{\sigma}_{t|t-1}^{rvd}$ [m] are the average and standard deviation of the vehicle position predicted by the Kalman filters at timestep t [s], and v_t [km/s], σ_{v_t} [km/s] are average and standard deviation of the vehicle velocity at timestep t [s], and $\frac{5}{18}$ is a term to convert a vehicle velocity from [km/h] to [m/s].

The vehicle position (average $\hat{x}_{t_0}^{rvd}$ [m] and standard deviation $\hat{\sigma}_{t_0}^{rvd}$ [m]) at timestep t_0 [s] is defined as the position received from the roadside vehicle detector, and hence is given by

$$\hat{x}_{t_0}^{rvd} = x_0^{rvd}, \quad (8)$$

$$\hat{\sigma}_{t_0}^{rvd} = \sigma_0^{rvd}. \quad (9)$$

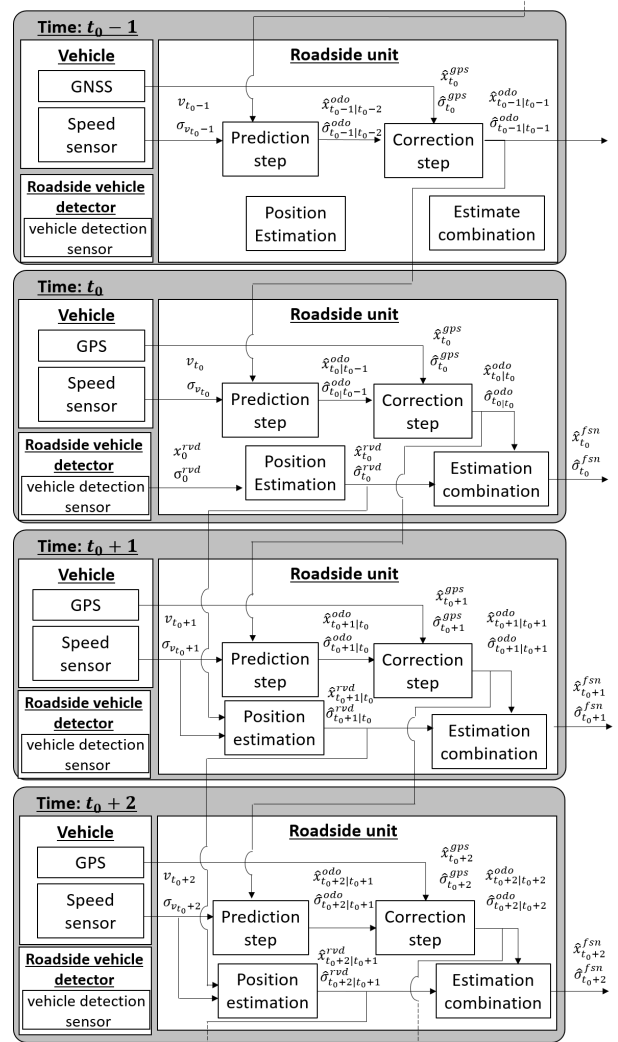


Figure 8. Flow diagram showing the steps performed to estimate the vehicle's position.

where x_0^{rvd} [m] and σ_0^{rvd} [m] are average and standard deviation, respectively, of the vehicle position received from the roadside vehicle detector.

Finally, the two vehicle position estimates are combined using a statistical approach proposed by Duffin [10], which is based on Bayes' Rule and Kalman filters. This approach simply combines the two Gaussian distribution as follows.

Estimate combination:

$$\hat{x}_t^{fsn} = \hat{x}_{t|t}^{odo} + \frac{\left(\hat{\sigma}_{t|t}^{odo}\right)^2}{\left(\hat{\sigma}_{t|t}^{odo}\right)^2 + \left(\hat{\sigma}_t^{rvd}\right)^2} \left(\hat{x}_t^{rvd} - \hat{x}_{t|t}^{odo}\right), \quad (10)$$

$$\left(\hat{\sigma}_t^{fsn}\right)^2 = \left\{1 - \frac{\left(\hat{\sigma}_{t|t}^{odo}\right)^2}{\left(\hat{\sigma}_{t|t}^{odo}\right)^2 + \left(\hat{\sigma}_t^{rvd}\right)^2}\right\} \left(\hat{\sigma}_{t|t}^{odo}\right)^2. \quad (11)$$

where \hat{x}_t^{fsn} [m] and $\hat{\sigma}_t^{fsn}$ [m] are average and standard deviation of the vehicle position obtained by combining the two estimates.

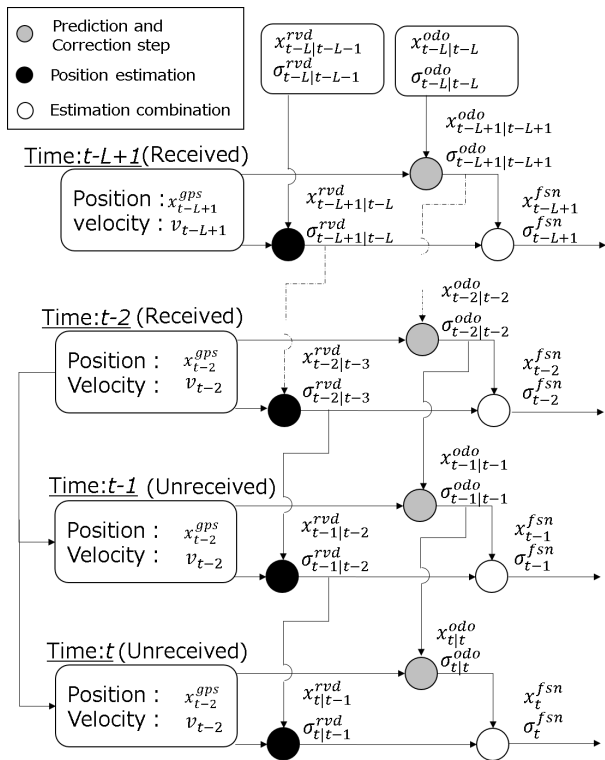


Figure 9. Overview of our communication delays compensation method.

B. Communication delays compensation

Since communication delays inevitable occur when exchanging information over wireless networks, it is necessary to take account for them when estimating the vehicle positions. Here, we use Kagami et al.'s approach, which involves modified Kalman filters that accounts for communication delays [11]. This method retroactively calculates prior positions and velocities when older data is received, up to a predetermined maximum communication delay. However, the modified Kalman filters' model Kagami et al.'s proposed is a multidimensional state space model. In this study, the communication delays compensation is only used the concept and Kalman filters' model was changed to a one-dimensional CV (Constant Velocity) model.

Figure 9 illustrates our method of compensating for communication delays. Here, L [s] is the maximum communication delay, $t-L$ [s] is L timesteps after the vehicle passed through the gate, and the roadside units did not receive any position and velocity information from the vehicle at timesteps $t-1$ and t [s]. The data is received at timestep $t-2$ [s], and the roadside unit uses this to retroactively calculate the vehicle positions and velocities at timesteps $t-1$ and t [s], working back from the present time to the predetermined maximum communication delay.

The vehicle position is estimated using (1)–(11) at each time. The vehicle's position is estimated based on the estimate from the previous time step and the each time vehicle position and velocity information. Finally, the two vehicle position estimates are combined.

IV. EVALUATION EXPERIMENTS

In this section, our vehicle position estimation method is evaluated using a series of simulations, conducted both with

TABLE I. SPECIFICATIONS OF THE PC USED FOR THE SIMULATIONS.

CPU	Intel Core i9-9900X @ 3.50GHz
Memory	64 GB
Storage	Samsung MZVLB1T0HALR-00000

TABLE II. PARAMETERS OF THE GAUSSIAN WHITE NOISE MODEL.

GNSS error	σ_w
Low	3
Medium	6
High	9

TABLE III. SPECIFICATIONS OF THE GNSS USED IN THE EXPERIMENT.

GNSS chip	UBX-M8030-KT (u-blox)
Receiver type	GPS, QZSS, GLONASS
Tracking sensitivity	-167[dBm]
Horizontal position accuracy	2.0[m]
Internal antenna	Dielectric antenna (25x25x4[mm])

TABLE IV. PARAMETERS OF THE GAUSS-MARKOV RANDOM PROCESS MODEL.

	σ_a	σ_r	β
Case 1	0.2020	0.0027	1/600
Case 2	0.1030	0.3160	1/600

and without communication delays. Here, we used Matlab R2019a. Table I shows that the specifications of PC used for simulation.

A. Environment without communication delays

In this experiment, the position estimation accuracy was evaluated in an environment where the communication delays were assumed to be negligible. Here, our proposed method (labeled as "Fusion" below) was compared with one that simply applies Kalman filters to the in-vehicle sensor data (labeled as "GNSS only").

In this simulation, a vehicle drove from the start point at $x = -100$ [m] toward the merging point at a speed of 80 [km/h]. The roadside vehicle detector was installed at $x = 0$ [m]. The standard deviations of the vehicle's center position and velocity were set to $\sigma_0^{rvd} = 0.5$ [m] and $\sigma_{v_t} = 5$ [km/s]. The vehicle sent its position and velocity to the roadside unit every 100[ms], and the roadside unit also estimated the vehicle's position every 100[ms]. The vehicle acquired its position from a GNSS device, and we considered the two models of GNSS position error, namely a Gaussian white noise model and a Gauss-Markov random process model, as used by a previous study [5]. There are described below, and the simulation was repeated six times for each GNSS position error models.

1) *Gaussian white noise model*: This is given by

$$x_t^{gps} = x_t + w_t. \quad (12)$$

where x_t is the actual vehicle position and w_t is Gaussian white noise, i.e., $w_t \sim N(0, \sigma_w)$. Here σ_w set as in Table II. σ_w in Table II are set from a trial experiment using a general-purpose GNSS sensor. The specifications of the GNSS used in the experiment is Table III. When position data were acquired using the sensor at multiple points in Nagoya University, the most low value was $\sigma_w \approx 3$, the most high value was $\sigma_w \approx 9$. Thus the σ_w is set as 3 in the low GNSS error and the σ_w is set as 9 in the high GNSS error. As an intermediate value

TABLE V. COMPARISON OF POSITION ESTIMATION METHODS.

Gaussian white noise model (Low GNSS position error)	Average [m]	Standard deviation [m]	
	GNSS only	0.298	0.182
	Fusion	0.238	0.030
Gaussian white noise model (Medium GNSS position error)	Average [m]	Standard deviation [m]	
	GNSS only	0.360	0.290
	Fusion	0.260	0.052
Gaussian white noise model (High GNSS position error)	Average [m]	Standard deviation [m]	
	GNSS only	0.467	0.461
	Fusion	0.274	0.085
Gauss–Markov random process model (Case 1)	Average[m]	Standard deviation[m]	
	GNSS only	1.681	0.907
	Fusion	1.280	0.591
Gauss–Markov random process model (Case 2)	Average [m]	Standard deviation [m]	
	GNSS only	0.691	0.467
	Fusion	0.477	0.315

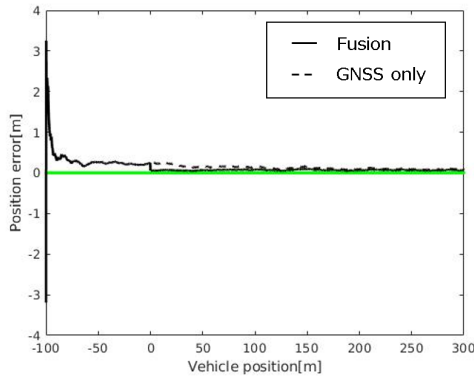


Figure 10. Position error versus true position (Gaussian white noise model with low GNSS position error).

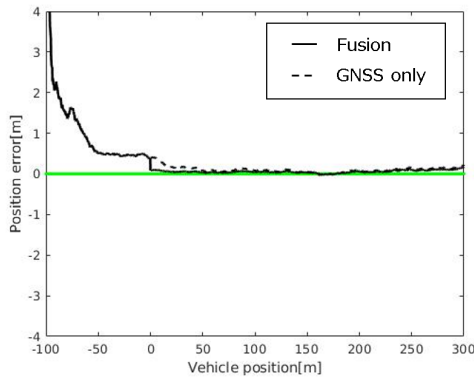


Figure 11. Position error versus true position (Gaussian white noise model with medium GNSS position error).

between the high and low GNSS error, σ_w is set as 6 in the medium GNSS error.

2) *Gauss–Markov random process model*: This is given by the following equations [14]:

$$m_t = e^{-\beta dt} m_{t-1} + g_t, \quad (13)$$

$$n_t = m_t + r_t, \quad (14)$$

$$x_t^{gps} = x_t + 0.9n_t. \quad (15)$$

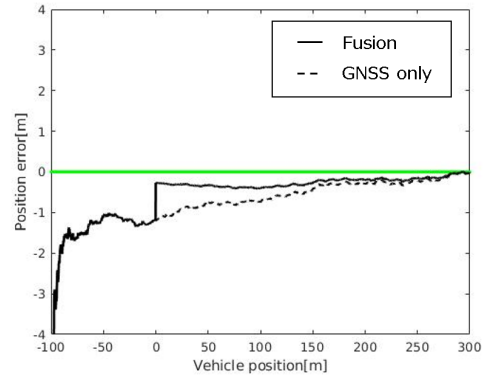


Figure 12. Position error versus true position (Gaussian white noise model with high GNSS position error).

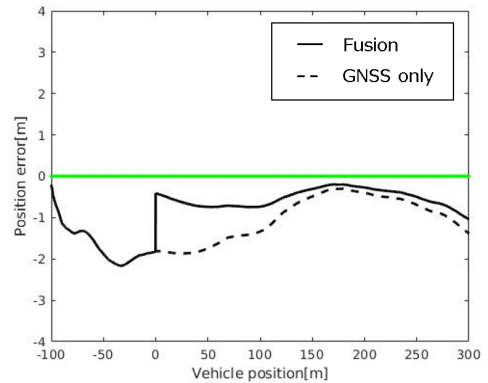


Figure 13. Position error versus true position (Gauss–Markov random process model, Case 1).

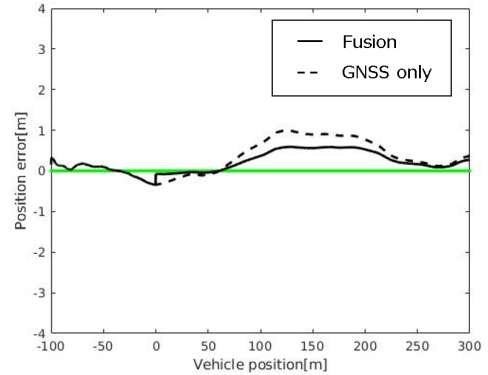


Figure 14. Position error versus true position (Gauss–Markov random process model, Case 2).

Here, represents time–correlated noise with time constant β and Gaussian white noise g_t , i.e., $g_t \sim N(0, \sigma_g)$. In addition, n_t is the total noise, composed of m_t and uncorrelated noise r_t , i.e., $r_t \sim N(0, \sigma_r)$. As in the previous study [5], σ_g , σ_r , and β were set as in Table IV. The case2 GNSS error is worse than the case1 in the paper [5].

B. Environment with communication delays

In this experiment, our communication delays compensation method is evaluated by comparing the performance our method (called “Fusion with DC” below) with those of two

TABLE VI. EVALUATION OF OUR COMMUNICATION DELAYS COMPENSATION METHODS.

	Average [m]	Standard deviation [m]
GNSS only without DC	-2.420	0.612
Maximum communication delay of 0.10[s]		
GNSS only with DC	-0.471	0.527
Fusion with DC	-0.248	0.065
Maximum communication delay of 0.12[s]		
GNSS only with DC	-0.410	0.411
Fusion with DC	-0.246	0.059
Maximum communication delay of 0.14[s]		
GNSS only with DC	-0.380	0.362
Fusion with DC	-0.234	0.063

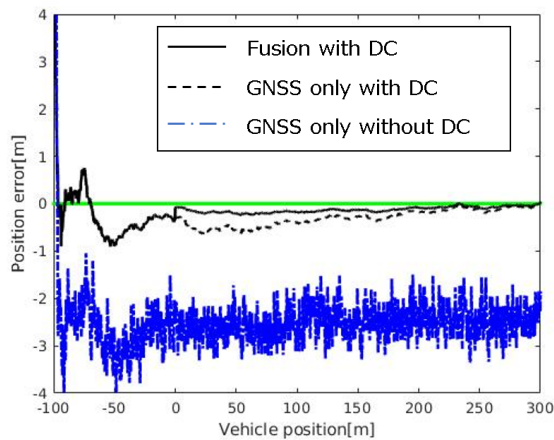


Figure 16. Evaluation of our communication delays compensation method (maximum communication delay of 0.12[s]).

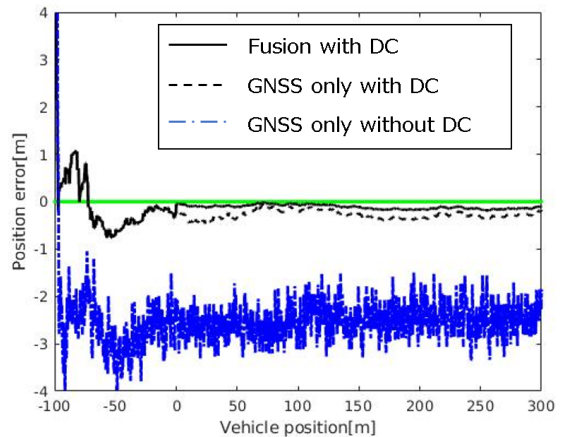


Figure 15. Evaluation of our communication delays compensation method (maximum communication delay of 0.10[s]).

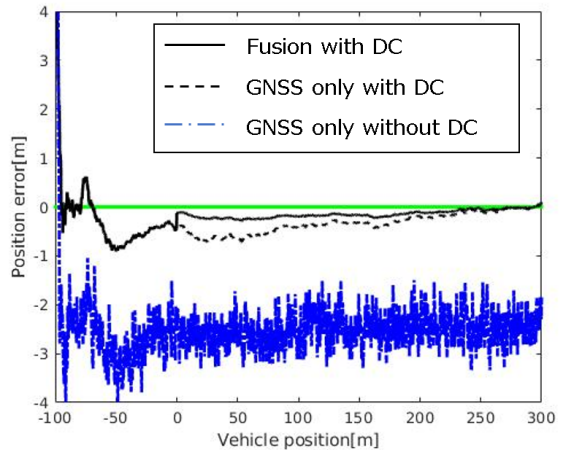


Figure 17. Evaluation of our communication delays compensation method (maximum communication delay of 0.14[s]).

other methods.

The first method (labeled as “GNSS only without DC”) estimates the vehicle’s position by applying Kalman filters to the in-vehicle sensor data without compensating for communication delays. This only uses the most recent position and velocity information received, ignoring older, delayed data. The second method (labeled as “GNSS only with DC”) is similar, but adds communication delay compensation.

Here, the communication delays were represented by Gaussian white noise, i.e., $N(\bar{d}, \sigma_d^2)$ \bar{d} was set to 96.130[ms] (following previous study [9]) and σ_d was set to 2[ms]. We considered three possible maximum communication delays, namely 0.10, 0.12, and 0.14[s], and repeated each simulation six times.

V. RESULTS

A. Position estimation

The simulation results are shown in Table V, and Figures 10-14 shows how the position error changed with the vehicle’s position. Here, the horizontal axis represents the true vehicle position, while the vertical axis represents the

position error, namely the difference between the true and estimated vehicle positions. When the position error is positive (negative), the vehicle’s estimated position is ahead of (behind) its true position.

As Table V shows the average and standard deviation of the position error are both lower for our “Fusion” method than for “GNSS only.” In Figures 10-14, we see that, when the vehicle passed through the gate and it became possible to obtain its position accurately, the position error of the “Fusion” method dropped sharply, becoming much lower than that of “GNSS only.” This demonstrates that the proposed position estimation method can be significantly more accurate than “GNSS only.”

B. Communication delays compensation

The simulation results are shown in Table VI, while Figures 15-17 show how the position error changed with the vehicle’s position, the horizontal axis represents the true vehicle positions, while the vertical axis represents the position error, defined as before.

As Table VI shows, both the average and standard deviation of the position error were lower for our “Fusion with DC” method than for the other approaches. In addition, the errors

were lower for “GNSS only with DC” than for “GNSS only without DC,” and were significantly lower for “Fusion with DC” than for the other methods when the maximum communication delay time was 0.14 [s]. We believe this is because the amount of data that had to be discarded, due to not being received within the maximum communication delay time, decreased as the maximum communication delay time increased.

In Figures 15-17, the position error is always negative for the “GNSS only without DC” method because the latest information received from the vehicle was out-of-data due to communication delays. The fact that the errors are smaller for both “GNSS only with DC” and “Fusion with DC” confirms that our communication delays compensation method performed well. In addition, the fact that the position errors are lower for our “Fusion with DC” method than for “GNSS only with DC” confirms that our proposed method can estimate the vehicle position more accurately than “GNSS only” in an environment with communication delays.

VI. CONCLUSION

In this paper, we have proposed a vehicle position estimation method that combines roadside vehicle detector and in-vehicle sensors. We have demonstrated that the proposed method can estimate vehicle positions more accurately than only using in-vehicle sensors. We have also confirmed that our communication delay compensation method can perform well. Since our method can estimate vehicle positions accurately in environments with communication delays, it is more suitable for managing traffic and controlling merging at junctions.

In future work, we will explore several topics. First, in order to evaluate our proposed method in practice, we will have to consider vertical movement. Since LTE introduces longer communication delays than DSRC does, we will also need to confirm that our communication delay compensation technique can perform well for LTE. Third, communication delays are influenced by various factors, such as the number of vehicles, building, and so on, so we will need to confirm that our communication delay compensation method is also effective in practice. Finally, the proposed method can be applied while the delay occurs according to a specific distribution. The communication delay distribution tendency changes drastically with the number of increasing vehicles. Thus, it is necessary to consider a method that can handle it even if the communication delay distribution tendency is changed.

ACKNOWLEDGMENT

This work was supported by JST-OPERA Program Grant Number JPMJOP1612, Japan.

REFERENCES

- [1] T. Abbas, L. Bernado, A. Thiel, C. F. Mecklenbräuker, and F. Tufvesson, “Measurements based channel characterization for vehicle-to-vehicle communications at merging lanes on highway,” In *Proceedings of the 5th International Symposium Wireless Vehicular Communications(WiVeC) June 2–3, 2013, Dresden, Germany*. IEEE, Jun. 2013, pp.1–5, ISBN: 978-1-4673-6339-6, URL: <https://ieeexplore.ieee.org/abstract/document/6698241> [retrieved: 12, 2019].
- [2] B. N. Janson, W. Awad, J. Robles, J. Kononov, and B. Pinkerton, “Truck accidents at freeway ramps: data analysis and high-risk site identification,” *Journal of Transportation and Statistics*, vol. 1, pp. 75–92, January, 1998, ISSN: 1094-8848.

- [3] H. Cui et al., “Early ramp warning using vehicle behavior analysis,” *Soft Computing*, vol. 22, pp. 1421–1432, March, 2018, ISSN: 1432-7643.
- [4] V. Milanés, J. Godoy, J. Villagra, and J. Perez, “Automated On-Ramp Merging System for Congested Traffic Situations,” *IEEE Transactions on Intelligent Transportation Systems*, vol. 12, pp. 500–508, June, 2011, ISSN: 1524-9050.
- [5] F. C. Chou, S. E. Shladover, and G. Bansal, “Coordinated merge control based on V2V communication,” In *Proceedings of the Vehicular Networking Conference (VNC) December 8–10, 2016, Ohio, USA*. IEEE, Dec. 2016, pp.1–8, ISBN: 978-1-5090-5197-7, ISSN: 2157-9865, URL: <https://ieeexplore.ieee.org/document/7835933> [retrieved: 12, 2019].
- [6] S. Hirai et al., “AHS Safety Service Utilizing an ITS On-Board Unit for Driving Support in Merging Sections,” *14th World Congress on ITS*, pp. 1–8, October, 2007.
- [7] “Start of Field Operational Tests of Autonomous Driving in Tokyo Waterfront Area,” URL: http://www.soumu.go.jp/menu_news/s-news/01kiban14_02000404.html [retrieved: 12, 2019].
- [8] Y. Morales and T. Tsubouchi, “DGPS, RTK-GPS and StarFire DGPS performance under tree shading environments,” In *Proceedings of IEEE international conference on integration technology (ICIT) March 20–24, 2007, Shenzhen, China*. IEEE, Mar. 2007, pp.519–524, ISBN: 1-4244-1091-6, URL: <https://ieeexplore.ieee.org/abstract/document/4290370> [retrieved: 12, 2019].
- [9] K. C. Deya, A. Rayamajh, M. Chowdhury, P. Bhavsar, and J. Martin, “Vehicle-to-vehicle (V2V) and vehicle-to-infrastructure (V2I) communication in a heterogeneous wireless network - Performance evaluation,” *Transportation Research Part C*, vol. 68, pp. 168–184, April, 2016.
- [10] W. Anderson and R. Duffin, “Series and parallel addition of matrices,” *Journal of Mathematical Analysis Applications*, vol. 26, pp. 576–594, 1969.
- [11] S. Kagami and M. Ishikawa, “A sensor selection method considering communication delays,” In *Proceedings of IEEE International Conference on Robotics and Automation(ICRA) April 26–May 1, 2004, LA, USA*. IEEE, May. 2001, pp.206–211, ISBN: 0-7803-8232-3, ISSN: 1050-4729, URL: <https://ieeexplore.ieee.org/document/13071529> [retrieved: 12, 2019].
- [12] “Start of joint research on information provision to support autonomous driving,” URL: <http://www.nilim.go.jp/lab/bcg/kisya/journal/kisya20180119.pdf> [retrieved: 12, 2019].
- [13] F. Sivrikaya and B. Yener, “Time synchronization in sensor networks: a survey,” *IEEE network*, vol. 18, pp. 45–50, August, 2004.
- [14] Rankin J, “An error model for sensor simulation GPS and differential GPS,” In *Proceedings of of IEEE Position Location and Navigation Symposium (PLANS’94) April 11–15, 1994, Las Vegas, USA*. IEEE, Apr. 1994, pp.260–266, ISBN: 0-7803-1435-2, URL: <https://ieeexplore.ieee.org/document/303322> [retrieved: 12, 2019].